SCIENTIFIC REPORTS

OPEN

SUBJECT AREAS:
POLYMERS
ORGANIC LEDS
DISPLAYS
OPTOELECTRONIC DEVICES AND COMPONENTS

Received
16 July 2013

Accepted
11 September 2013

Published
27 September 2013

Correspondence and requests for materials should be addressed to K.C. (chochem@korea.ac.kr) or S.K. (sangsig@korea.ac.kr)

Stable Bending Performance of Flexible Organic Light-Emitting Diodes Using IZO Anodes

Kiyeol Kwak, Kyoungah Cho & Sangsig Kim

Department of Electrical Engineering, Korea University, Seoul 136-713, Korea.

We report luminescent characteristics and mechanical stability of a flexible organic light-emitting diode (FOLED) using an amorphous ZnO-doped In_2O_3 (*a*-IZO) anode with a low sheet resistance of 18.9 Ω/□ and a high optical transparency of 86%. The FOLED consisting of *a*-IZO/poly(3,4-ethylenedioxythiophene) poly(styrenesulfonate) (PEDOT:PSS)/poly[(9,9-di-n-octylfluorenyl-2,7-diyl)-alt-(benzo[2,1,3]thiadiazol-4,8-diyl)] (F8BT)/LiF/Al exhibits the efficient luminescent characteristics, which are nearly identical with the photoluminescence spectrum of the organic emitting material in our FOLED. This observation clearly indicates that the luminescent characteristics of the FOLED are solely ascribed to molecular *exciton* formation within the F8BT layer, since *exciplex* and charge transfer *exciton* formation are strictly suppressed by both tunneling/thermionic injection of holes at the PEDOT:PSS/F8BT interface and enhanced hole transport. Furthermore, the use of the considerably flexible *a*-IZO anode and PEDOT:PSS acting as a strain-relief buffering material enables good retention of the efficient luminescent characteristics of the FOLED even after continuous bending of up to 1000 times.

In recent years, flexible organic light-emitting diodes (FOLEDs) have emerged as one of the basic components in next-generation display systems owing to the evolution of portable electronic devices that require lightweight, bendable and unbreakable display devices[1–4]. To achieve the FOLEDs utilized in flexible display systems, it is essential to satisfy efficient luminescent characteristics and stable performance issues in the FOLED regardless of its repeated deformation. Over the past two decades, many studies have aimed at enhancing performance in OLEDs by employing multi-layer structures comprising organic semiconductors and a blended polymer as an organic emission layer (EML)[5–7]. However, OLEDs with multi-layer structures usually exhibit *exciplex* and/or charge transfer (CT) *exciton* formations at the interface resulting in inefficient luminescent properties, which originate from the offsets of the highest occupied molecular orbitals (HOMOs) and the lowest unoccupied molecular orbitals (LUMOs) between two organic semiconductors[8,9]. In order to design efficient FOLED with desirable and efficient luminescent properties, structural optimization should be considered together with the choice of appropriate materials in the FOLED. Herein, we propose a simple FOLED structure consisting of a EML made of poly[(9,9-di-n-octylfluorenyl-2,7-diyl)-alt-(benzo[2,1,3]thiadiazol-4,8-diyl)] (F8BT) and a hole transport layer (HTL) inserted between the flexible transparent anode and the EML. Poly(3,4-ethylenedioxythiophene) poly(styrenesulfonate) (PEDOT:PSS) is utilized here as a hole transporting material upon consideration of the work function of the anode and the HOMO/LUMO energy levels of F8BT[10,11]. In addition, the PEDOT:PSS layer effectively improves the hole injection toward the F8BT layer which is well-known as an n-type organic semiconductor and is a trapping for holes[12]. An amorphous ZnO-doped In_2O_3 (*a*-IZO) is chosen for our FOLED as the most appropriate anode material, because it has been strongly regarded as offering a very promising flexible transparent anode due to its remarkable mechanical flexibility as well as its excellent optical and electrical properties[10,13,14]. The choice of the flexible transparent anode in the FOLEDs is one of the crucial issues related to a stable performance retaining luminescent characteristics regardless of its repeated deformation. In this study, in order to realize the highly efficient and stable performance, we design a FOLED with a simple structure of *a*-IZO/PEDOT:PSS/F8BT/LiF/Al on the flexible plastic and investigate its luminescent and electrical characteristics, and mechanical stability. Figure 1 shows molecular structures of PEDOT:PSS (left) and F8BT (right) (Fig. 1(a)), and a schematic diagram of the FOLED constructed on the flexible plastic (Fig. 1(b)).

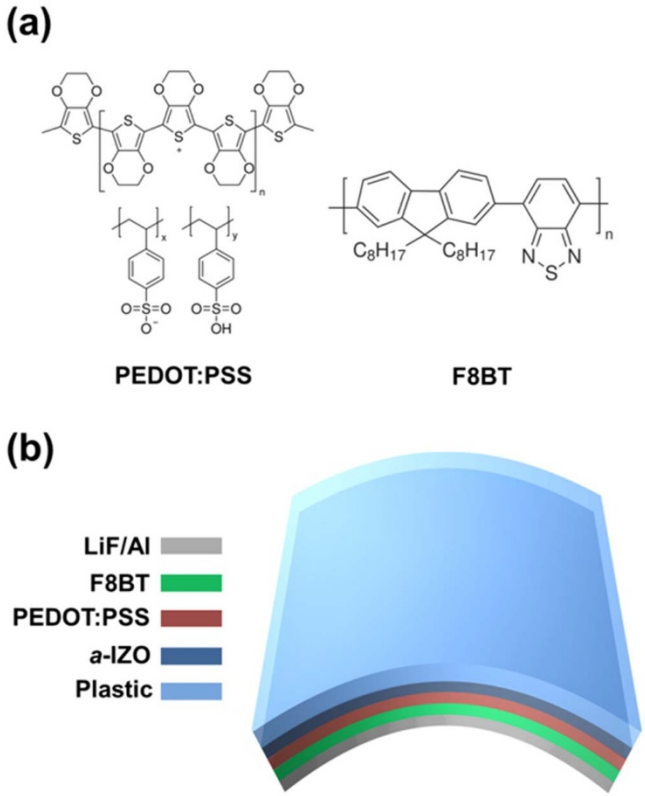

Figure 1 | (a) The molecular structures of PEDOT:PSS (left) and F8BT (right), and (b) a schematic diagram of the FOLED with the structure of *a*-IZO/PEDOT:PSS/F8BT/LiF/Al constructed on a flexible plastic substrate.

Results

The optical transmittance spectra show that the optical transparency of the *a*-IZO film on a poly-ether-sulfone (PES) substrate is as high as 86% at a wavelength of 550 nm and its average optical transparency in the visible range (400–700 nm) is 83% as plotted in Fig. 2. This excellent optical transparency is comparable to those of other flexible transparent anodes such as single-walled carbon nanotube (SWCNT) (~90%) and Ag NWs network (~86%) deposited on polycarbonate or polyethylene terephthalate substrates[15,16]. The sheet resistance of the *a*-IZO film measured in this work is as low as 18.9 Ω/□, and such a low sheet resistance allows for efficient hole injection from anode to organic semiconductor layers. From the optical transparency (T) and sheet resistance (R_{sh}) of the *a*-IZO film on the PES substrate, a figure of merits (Φ_{TC}) of the transparent anode can be calculated using Equation (1), which is suggested by Haacke[17].

$$\Phi_{TC} = \frac{T^{10}}{R_{sh}} \quad (1)$$

The Φ_{TC} value of the *a*-IZO film in this study is estimated to be $12.3 \times 10^{-3}\ \Omega^{-1}$, which is higher than those of other flexible transparent anodes[15,16,18–21], indicating that the *a*-IZO film is a promising anode material for good performance in FOLEDs.

We examine a ratio of sheet resistance change-to-initial sheet resistance ($|R - R_o|/R_o = \Delta R/R_o$) as a function of bending radius to find the maximum bending radius of our sputtered *a*-IZO film; note that R is the measured sheet resistance after cyclic bending and that R_o is the initial sheet resistance of the *a*-IZO film. And the thickness of the *a*-IZO film (~130 nm) is much thinner than that of the flexible plastic (~200 μm) in this study, so that it is reasonable to assume that the *a*-IZO film and the flexible plastic undergo a similar degree of mechanical strain. When the flexible substrate is bent with a bending radius (R_c), the amount of strain applied to the *a*-IZO film is estimated using Equation (2)[22];

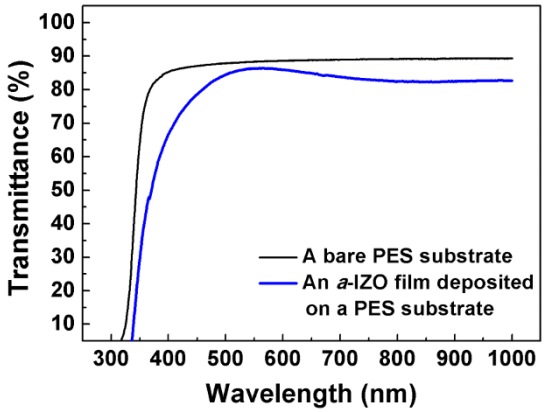

Figure 2 | **Optical transmittance curves of the bare PES substrate and the *a*-IZO film on the PES substrate.**

$$Strain(\%) = \frac{t_{film} + t_{plastic}}{2 \times R_c} \quad (2)$$

where t_{film} and $t_{plastic}$ are the thicknesses of the *a*-IZO film and the flexible plastic substrate, respectively. As shown in Fig. 3(a), the maximum bending radius of our *a*-IZO film is 10.5 mm since the sheet resistance of the *a*-IZO film remarkably increases at the bending radius of 7.8 mm corresponding to 1.25% of strain. Therefore, we investigate mechanical flexibility of the *a*-IZO film when the flexible substrate is bent with the maximum radius of 10.5 mm corresponding to 1% of strain. The ratio of sheet resistance change-to-initial sheet resistance ($|R - R_0|/R_o = \Delta R/R_o$) as a function of bending times (#) is evaluated as shown in Fig. 3(b). Although there are changes in the sheet resistance of the *a*-IZO film in a cyclic bending test, the sheet resistance of the *a*-IZO film, up to a bending cycle of 1000 times, is appropriate to be utilized as a transparent anode of FOLED. The inset of Fig. 3(b) shows a photograph of the *a*-IZO film on the flexible plastic substrate under the continuous bending test using the home-made bending machine. The optical profiler images of Figs. 3(c) and (d) exhibit the changes in the surface morphologies of the sputtered *a*-IZO films before and after the 1000 times cyclic bendings with a bending radius of 10.5 mm (corresponding to a bending strain of 1%), respectively. A few nano-scale cracks appear in the surface morphology as shown in Fig. 3(d), which is attributed to the difference in sheet resistance in a cyclic bending test.

Discussion

Table 1 lists several key parameters of flexible transparent films including the experimental results of this study, which are essential requirements for the construction of the FOLEDs. AuO_x has a much lower sheet resistance of ~6.0 Ω/□, but it has a poor optical transparency (<60%), so that it is unsuited to be used as flexible transparent anode for FOLEDs[18]. In contrast, SWCNT and PEDOT:PSS/SWCNT nanocomposite show the good mechanical flexibility as well as the high optical transparency, but they have inferior electrical properties which lead to inefficient injection of holes from anode to organic semiconductor layers due to their high sheet resistance[15,20]. In case of PEDOT:PSS and conducting polymer, they are not appropriate to be utilized as the flexible transparent anodes, because of their high sheet resistance and high ratio of sheet resistance change under the consecutive bending with a low strain[19,21]. In spite of the excellent optical and electrical properties, furthermore, the ratio of the sheet resistance change of the Ag NW network increases to about 3 for the 250 bending times[16]. This observation indicates the poor mechanical flexibility of the Ag NW network under the continuous

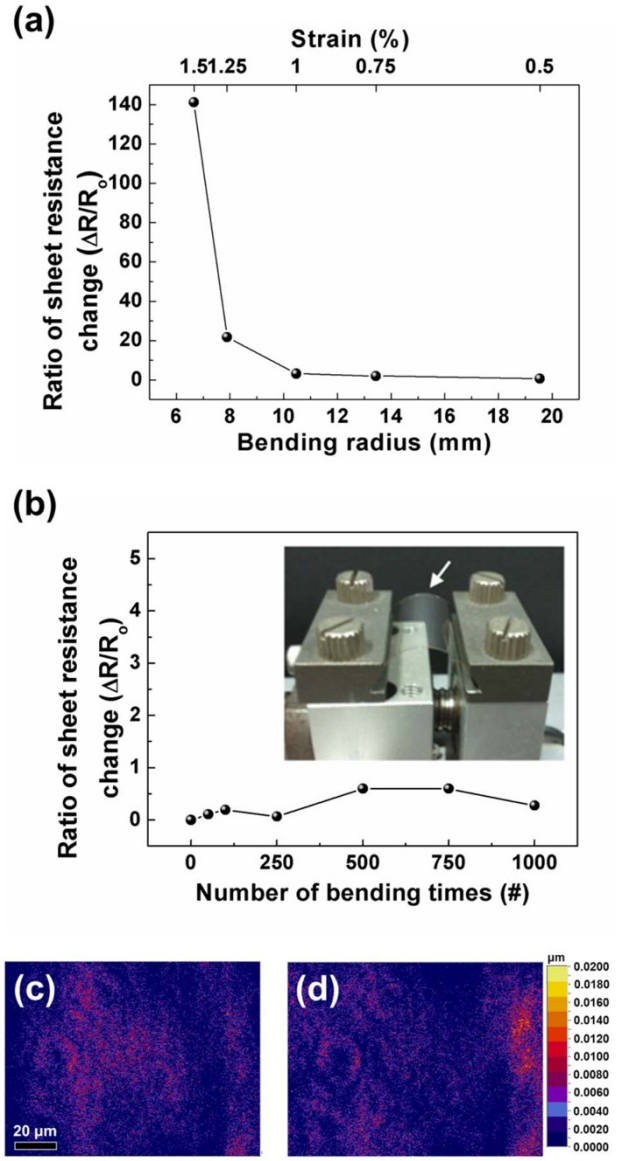

Figure 3 | Ratio of sheet resistance change ($\Delta R/R_o$) of the *a*-IZO film sputtered on a flexible plastic substrate (a) as a function of bending radius and (b) as a function of the number of bending times (#). And the optical profiler images of the *a*-IZO films (c) before and (d) after 1000 times cyclic bending test with a bending radius of 10.5 mm, respectively. The inset shows a photograph when the bending test for mechanical flexibility of the *a*-IZO film is performed with a home-made bending machine.

mechanical bending test, revealing its unsuitability as a flexible transparent anode for the FOLEDs. Compared with those flexible transparent anode films, the *a*-IZO film shows relatively superior properties in terms of sheet resistance, optical transparency, and mechanical flexibility. Hence, among flexible transparent anodes, the *a*-IZO anode sputtered in this work is the most appropriate flexible transparent anode for realizing efficient and stable performance in the FOLED.

In both of a normalized photoluminescence (PL) spectrum taken from the spin-coated F8BT layer (black) and a normalized electroluminescence (EL) spectrum of the fabricated FOLED at a biased voltage of 7.5 V (olive), the green colored emission is dominant as shown in Fig. 4(a); a photograph of the green colored emission from the FOLED in the dark is presented in the inset. The green colored emission is typically associated with keto-emission *via* the keto-defects in F8BT[23]. The peak position (535 nm) and the full width

Table 1 | Several key parameters of flexible transparent films

Anode	Sheet resistance (Ω/□)	Transmittance@ 550 nm (%)	Work function (eV)	Figure of Merits ($10^{-3}\,\Omega^{-1}$)	Mechanical flexibility			Ref.
					Strain (%)	Number of bending times (#)	Ratio of sheet resistance change ($\Delta R/R_o$)	
a-IZO	18.9	86	5.2	12.3	1	1000	≤0.6	this study and10
AuO_x	6.0	60	5.7	1	N/A	N/A	N/A	18
SWCNT	300	90	4.7–5.2	1.2	1.2	1000	≤0.1	15
PEDOT:PSS	296	82	5.0	0.4	0.4	700	1.8	19
PEDOT:PSS/SWCNT nanocomposite	40–60	85	5.0	4.9	0.9	1600	≤0.1	20
Conducting polymer	2000	80–85	4	0.1	0.3	1500	≤0.5	21
Ag NW network	30	86	4.5	7.7	3.4	250	≤3	16

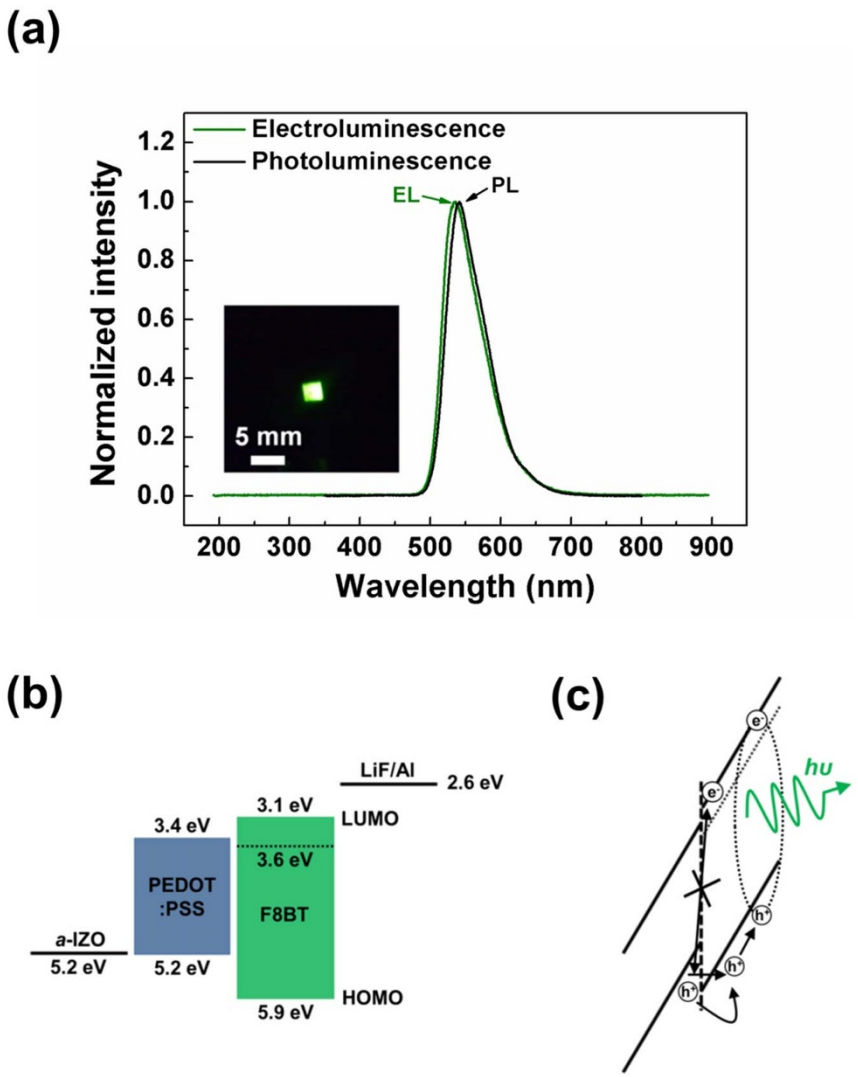

Figure 4 | (a) The normalized PL spectrum of the F8BT layer, and the normalized EL spectrum of the FOLED, when a biased voltage of 7.5 V is applied; the inset is a photograph of the green colored emission from the FOLED in the dark. (b) Schematic energy diagram of the FOLED with a structure of *a*-IZO/PEDOT:PSS/F8BT/LiF/Al in a thermal equilibrium state and (c) the charge carriers injection mechanism at the PEDOT:PSS/F8BT interface when an turn-on voltage of ~4 V is applied to the FOLED.

at half maximum (FWHM) (66 nm) of the EL spectrum of the FOLED are surprisingly identical to those of the PL spectrum obtained from the spin-coated F8BT layer, corresponding to 541 and 66 nm, respectively. This observation clearly reveals that the luminescent characteristics of the FOLED are solely ascribed to molecular *exciton* formation within the F8BT layer, implying a highly efficient performance in the FOLED. The phenomenon has rarely been observed in the field of the OLED, which implies a well-optimized structure of our FOLED without *exciplex* emission.

Considering the energy diagram of our FOLED as illustrated in Fig. 4(b), it is possible that our FOLED shows *exciplex* emission ascribed to interfacial *exciplex* states formed at the PEDOT:PSS/F8BT interface because the HOMO offset of ~0.7 eV between PEDOT:PSS and F8BT leads to accumulation of holes at the PEDOT:PSS/F8BT interfacial potential barrier. Actually, G. Bernardo *et al.* reported the presence of an emissive *exciplex* between F8BT and PEDOT:PSS through the photophysical characterization using PL, PL excitation spectra and fluorescence decay measurement[24]. And, in the EL spectrum of their previous study, two peaks were observed at 550 and 574 nm and the emission broadening was apparent from the difference in the FWHM of EL (~87 nm) and PL (~72 nm) spectra. However, against our expectation, no evidence for the *exciplex* emission at the PEDOT:PSS/F8BT interface is observed in the EL spectrum of the FOLED (Fig. 4(a)). The EL spectrum without *exciplex* emission can be understood as follows. When an electric field higher than the tunneling threshold voltage is applied to the FOLED, holes easily transport *via* tunneling and/or thermionic injection to the F8BT layer, so that molecular *exciton* formation is enhanced within the F8BT layer as depicted in Fig. 4(c)[25]. The higher turn-on voltage of ~4 V than the tunneling threshold voltage of ~3.8 V in this study demonstrates that tunneling and/or thermionic injection of holes at the PEDOT:PSS/F8BT interface are associated with the efficient luminescent characteristics of the FOLED. In addition, the absence of any CT emission in the EL spectrum (Fig. 4(a)) can be explained by the filling of sub-bands localized in the F8BT layer.

In comparison with the luminescent properties of OLEDs consisting of F8BT as the EML, the structure of *a*-IZO/PEDOT:PSS/F8BT/LiF/Al in this study shows the most efficient luminescent characteristics as demonstrated in Table 2[23,24,26,27]. There are three valid reasons for the better performance of our FOLED compared with other F8BT based OLEDs: i) the PEDOT:PSS layer, ii) the *a*-IZO anode, and iii) the LiF/Al cathode. As mentioned above, PEDOT:PSS used as the HTL allows more holes to be trapped in the F8BT layer, and

Table 2 | Luminescent characteristics of OLEDs consisting of F8BT as the EML

Structure	EL spectrum		PL spectrum		Comparison		Ref.
	Peak position (nm)	FWHM (nm)	Peak position (nm)	FWHM (nm)	ΔPeak position (nm)	ΔFWHM (nm)	
a-IZO/PEDOT:PSS/F8BT/LiF/Al	535	66	541	66	6	0	this study
c-ITO/PEDOT:PSS/F8BT/Ca/Al	~541	~62	~562	~65	~21	~3	26
c-ITO/PEDOT:PSS/F8BT/Mg	~550 ~574	~87	~550	~72	~0 ~24	~25	24
c-ITO/F8BT/Ca/Al	~572	~88	~530	~70	~42	~18	23
c-ITO/F8BT/Ca/Al	~560	~67	~533	~100	~27	~33	27

consequently the balanced electron and hole current in the F8BT layer contributes to efficient molecular *exciton* formation within the F8BT layer[28]. Furthermore, we consider our FOLED utilizing an *a*-IZO anode and LiF/Al cathode to be superior to others using a crystalline ITO (*c*-ITO) anode and Ca/Al cathode, since the amorphous structure of our *a*-IZO anode reduces the strain applied to the organic semiconductor layers relatively more than the *c*-ITO anode and LiF/Al cathode, which helps in minimizing non-radiative emission and/or maximizing out-coupling in the FOLED[29,30]. The FOLED structure proposed in this study, *a*-IZO/PEDOT:PSS/F8BT/LiF/Al, is ideal for demonstrating the luminescent property of the F8BT used as the organic emitting material in our FOLED.

A current density *versus* voltage (*J*-*V*) curve of our FOLED is plotted in Fig. 5 in log *J*-log *V* scale and reveals the existence of three regions associated with different types of charge carrier transport mechanisms. At lower voltage than an turn-on voltage of about 4 V, the current of charge carriers in region (i) follows Ohm's law ($J \propto V$) with a low leakage current density ($<1\ \mu A/cm^2$). This low leakage current density is associated with insertion of the PEDOT:PSS between the F8BT layer and the *a*-IZO anode. The PEDOT:PSS layer spin-coated on the *a*-IZO anode plays the role of a buffer layer relaxing the roughness of the surface before the deposition of the F8BT layer. As a result, the low leakage current density reduces the electrical short between the F8BT layer and the *a*-IZO anode[31]. In region (ii), where the biased voltage range from about ~4 to ~6 V, the relation of $J \propto V^4$ indicates the mechanism of a trap-filled limited current (TFLC) which means that sub-bands in the F8BT layer are filled and the injected charge carriers are free to move[32]. This TFLC is basically concerned with luminescent properties of the FOLED that are nearly identical to the PL spectrum of the spin-coated F8BT layer as exhibited in Fig. 4(a), because the CT *exciton* formation ascribed to interfacial CT states localized at the PEDOT:PSS/F8BT interface is strictly limited by filling of sub-bands

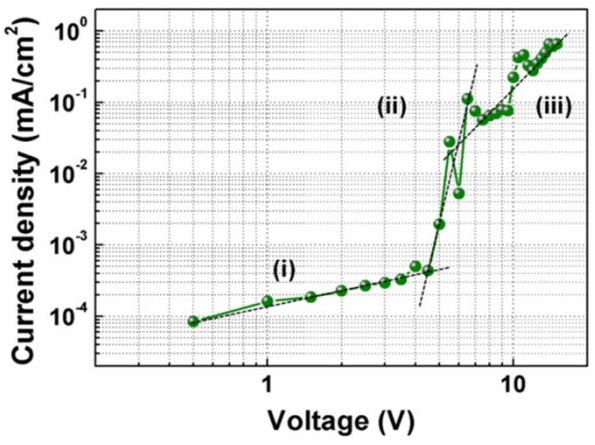

Figure 5 | A log *J*-log *V* plot of the FOLED with the structure of *a*-IZO/PEDOT:PSS/F8BT/LiF/Al.

localized in the F8BT layer. Region (iii) shows the typical characteristics for a trap-free space charge limited current ($J \propto V^2$) above the biased voltage of ~6 V[33].

In order to evaluate the mechanical flexibility of our FOLED, the ratio of intensity change-to-initial intensity ($|I - I_o|/I_o = \Delta I/I_o$) and the peak position change of the EL spectrum at a biased voltage of 7.5 V were examined through a continuous bending test with a strain of 1% up to 1000 times. The intensity and the peak position of the EL spectrum obtained from the FOLED were measured at 50, 100, 250, 500, 750, and 1000 bending times, respectively. The intensity and the peak position of the EL spectrum are changed a lot for the first 50 bending cycles, and then remain stable for the 1000 bending cycles as shown in Fig. 6(a). This clearly reveals excellent stable performance of the FOLED attributable to the good mechanical flexibility of the *a*-IZO anode and the strain-buffering effect of the PEDOT:PSS layer used as the HTL. Polymers such as the PEDOT:PSS layer have usually been employed in the field of flexible optoelectronics in order to relieve the strain applied to the devices[34,35]. The strain-buffering effect of PEDOT:PSS is confirmed from comparison with EL spectra of the FOLED in flat and bent states with a strain of 1% (as shown in Fig. 6(b)). The luminescent properties of the FOLED in flat and bent states with a bending radius of 10.5 mm (a bending strain of 1%) are nearly identical. The peak position of the EL spectrum of the FOLED in the bent state is completely identical to that in the flat state, which clearly demonstrates that the electronic structure of the F8BT layer is not changed even under a strain of 1%, by virtue of the strain-buffering effect of the PEDOT:PSS layer. The FOLED designed in this study has excellent flexibility properties, resulting from the good mechanical flexibility of the *a*-IZO anode and the efficient buffering role of the PEDOT:PSS layer.

In conclusion, we demonstrate and examine the luminescent characteristics and mechanical stability of a FOLED consisting of solution-processed PEDOT:PSS and F8BT layers on the *a*-IZO anode with a high optical transparency of 86%. The low sheet resistance of 18.9 Ω/□ of the *a*-IZO film is nearly constant under a cyclic bending test with a strain of 1%, which reveals its suitability as a flexible transparent anode to realize stable performance in the FOLED regardless of its repeated deformation. The EL spectrum of the FOLED is nearly identical to the PL spectrum of the spin-coated F8BT layer. These efficient luminescent characteristics of the FOLED originate from molecular *exciton* formation within the F8BT layer, since the FOLED is clearly optimized with the structure of *a*-IZO/PEDOT:PSS/F8BT/LiF/Al. Moreover, this efficient performance in the FOLED is retained well even after the cyclic bending test performed up to 1000 times, which is attributable to the good mechanical flexibility of the sputtered *a*-IZO anode and the strain-buffering effect of the PEDOT:PSS layer. Our results reveal that FOLEDs with efficient and stable performance are made with FOLED structures suitable for organic emitting materials. Both structural optimization and the choice of materials in the FOLEDs are determining factors in order to realize efficient and stable performance FOLED for the development of future flexible display systems.

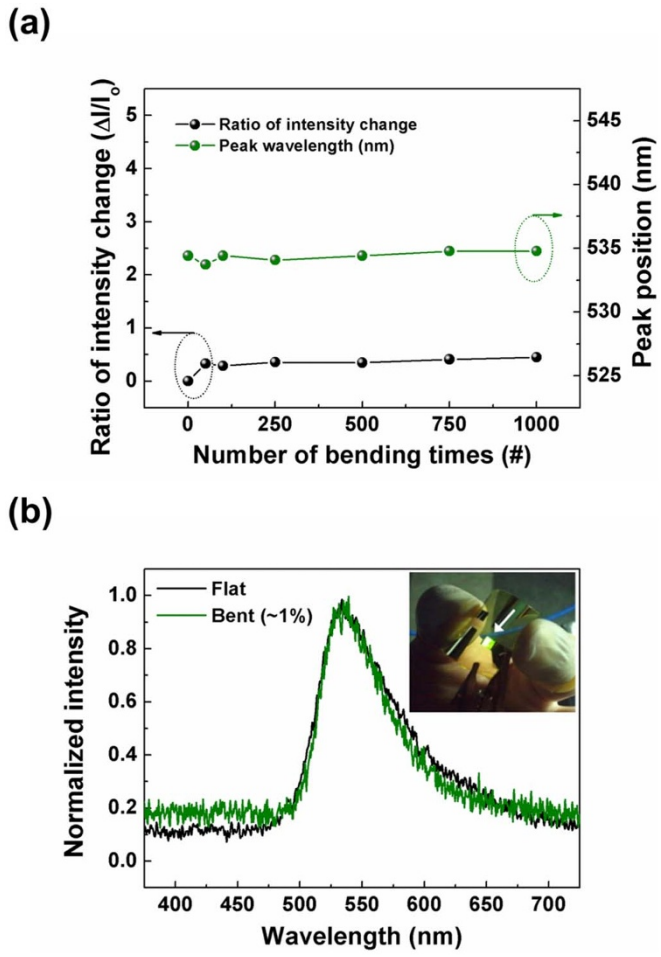

Figure 6 | (a) Ratio of intensity change ($\Delta I/I_o$) (left) and peak position (right) of the EL spectrum obtained from the FOLED measured as a function of the number of bending times (#) up to 1000 times and (b) the normalized EL spectra of the FOLED in flat and bent states, with a bending radius of 10.5 mm (a bending strain of 1%); inset shows a photograph of the green colored emission from the FOLED when it is in the bent state.

Methods

Fabrication of the FOLEDs. The PES substrate with a thickness of 200 μm (i-components Co., Ltd.) was used as a flexible substrate (25 × 25 mm^2) due to its excellent optical transparency and mechanical flexibility[14]. PEDOT:PSS and F8BT were purchased from HC Stark (Clevios AI 4083) and Sigma-Aldrich, respectively. The FOLED consisting of PEDOT:PSS and F8BT was constructed on the flexible plastic according to the following procedures. At first, *a*-IZO film was patterned on the flexible plastic by photolithography process using a photo mask, and sputtered from an IZO target (10 wt.% ZnO-doped In_2O_3) at room temperature under pure ambient Ar. The *a*-IZO film was then treated with UV-ozone for 20 minutes to improve the hydrophilic property and to remove organic contaminants such as photoresist materials[36,37]. Moreover, the UV-ozone treatment enhances the injection efficiency of holes for a high work function anode[38]. After the UV-ozone treatment, the PEDOT:PSS layer was formed on the *a*-IZO anode by spin-coating method, and then dried on a hot plate at a temperature of 90°C for 30 minutes, in order to remove solvent. F8BT dissolved in *p*-xylene (10 mg/ml) was spin-coated on the PEDOT:PSS layer, and dried at 70°C for 30 minutes. Finally, LiF (1 nm) and Al (100 nm) as the cathode of the FOLED were deposited by thermal evaporation. The emission layer area of the fabricated FOLED was 3 × 3 mm^2.

Measurements. The optical transparency and sheet resistance of the *a*-IZO film sputtered on the PES substrate were measured by a spectrophotometer (Shimadzu UV-3101PC) and a four-point probe system (Advanced Instrument Technology CMT-series), respectively. And surface changes of the sputtered *a*-IZO film before and after the continuous bending test were obtained from the non-contacting optical profiler (Veeco NT-1100). The electrical characteristics of the fabricated FOLED were examined with a semiconductor parameter analyzer (Agilent 4155C). The PL spectrum of the spin-coated F8BT layer and the EL spectrum of the FOLED were taken with a spectrofluorophotometer (Shimadzu RF-5301PC) and a spectrophotometer (Ocean Optics USB2000plus), respectively. Mechanical bending tests of the *a*-IZO film and the fabricated FOLED were performed with a home-made bending machine[39]. All measurements were carried out in air at room temperature.

1. Park, B. & Jeon, H. G. Spontaneous buckling in flexible organic light-emitting devices for enhanced light extraction. *Opt. Express* **19**, A1117–A1125 (2011).
2. Koo, J.-R. *et al.* Flexible bottom-emitting white organic light-emitting diodes with semitransparent Ni/Ag/Ni anode. *Opt. Express* **21**, 11086–11094 (2013).
3. Yu, Z. *et al.* Highly Flexible Silver Nanowire Electrodes for Shape-Memory Polymer Light-Emitting Diodes. *Adv. Mater.* **23**, 664–668 (2011).
4. Wang, Z. B. *et al.* Unlocking the full potential of organic light-emitting diodes on flexible plastic. *Nat. Photonics.* **5**, 753–757 (2011).
5. Ruhstaller, B. *et al.* Simulating electronic and optical processes in multilayer organic light-emitting devices. *IEEE J. Sel. Top. Quant.* **9**, 723–731 (2003).
6. Oyston, S. *et al.* Enhanced electron injection and efficiency in blended-layer organic light emitting diodes with aluminium cathodes: new 2,5-diaryl-1,3,4-oxadiazole–fluorene hybrids incorporating pyridine units. *J. Mater. Chem.* **15**, 5164–5173 (2005).
7. Ma, D. *et al.* Novel Heterolayer Organic Light-Emitting Diodes Based on a Conjugated Dendrimer. *Adv. Funct. Mater.* **12**, 507–511 (2002).
8. Mazzeo, M. *et al.* Organic single-layer white light-emitting diodes by exciplex emission from spin-coated blends of blue-emitting molecules. *Appl. Phys. Lett.* **82**, 334–336 (2003).
9. Kim, J.-S., Seo, B.-W. & Gu, H.-B. Exciplex emission and energy transfer in white light-emitting organic electroluminescent device. *Synthetic Met.* **132**, 285–288 (2003).
10. Kim, H.-K. High-performance phosphorescent organic light-emitting diodes prepared using an amorphous indium zinc oxide anode film grown by box cathode sputtering. *Surf. Coat. Technol.* **203**, 652–656 (2008).
11. Qian, L. *et al.* Electroluminescence from light-emitting polymer/ZnO nanoparticle heterojunctions at sub-bandgap voltages. *Nano Today* **5**, 374–389 (2010).
12. Seeley, A. J. A. B., Friend, R. H., Kim, J.-S. & Burroughes, J. H. Trap-assisted hole injection and quantum efficiency enhancement in poly(9,9′ dioctylfluorene-alt-benzothiadiazole) polymer light-emitting diodes. *J. Appl. Phys.* **96**, 7643–7649 (2004).
13. Kang, J.-W. *et al.* High-Performance Flexible Organic Light-Emitting Diodes Using Amorphous Indium Zinc Oxide Anode. *Electrochem. Solid State Lett.* **10**, J75–J78 (2007).
14. Rim, Y. S., Kim, H. J. & Kim, K. H. Characteristics of indium zinc oxide films deposited using the facing targets sputtering method for OLEDs applications. *Thin Solid Films* **518**, 6223–6227 (2010).
15. Han, T. H. *et al.* Extremely efficient flexible organic light-emitting diodes with modified graphene anode. *Nat. Photonics* **6**, 105–110 (2012).
16. Zeng, X. Y., Zhang, Q. K., Yu, R. M. & Lu, C. Z. A New Transparent Conductor: Silver Nanowire Film Buried at the Surface of a Transparent Polymer. *Adv. Mater.* **22**, 4484–4488 (2010).
17. Haacke, G. New figure of merit for transparent conductors. *J. Appl. Phys.* **47**, 4086–4089 (1974).
18. Helander, M. G. *et al.* Oxidized gold thin films: an effective material for high-performance flexible organic optoelectronics. *Adv. Mater.* **22**, 2037–2040 (2010).
19. Wang, Y. *et al.* An efficient flexible white organic light-emitting device with a screen-printed conducting polymer anode. *J. Phys. D: Appl. Phys.* **45**, 402002 (2012).
20. Wang, G.-F., Tao, X.-M. & Wang, R.-X. Flexible organic light-emitting diodes with a polymeric nanocomposite anode. *Nanotechnology* **19**, 145201 (2008).
21. Huh, J. W. *et al.* Characteristics of organic light-emitting diodes with conducting polymer anodes on plastic substrates. *J. Appl. Phys.* **103**, 044502 (2008).
22. Lee, K. J. *et al.* A Printable Form of Single-Crystalline Gallium Nitride for Flexible Optoelectronic Systems. *Small* **1**, 1164–1168 (2005).
23. Yang, X. H. *et al.* Suppression of the Keto-Emission in Polyfluorene Light-Emitting Diodes: Experiments and Models. *Adv. Funct. Mater.* **14**, 1097–1104 (2004).
24. Bernardo, G. *et al.* Synergistic effect on the efficiency of polymer light-emitting diodes upon blending of two green-emitting polymers. *J. Appl. Phys.* **108**, 014503 (2010).
25. Morteani, A. C., Ho, P. K. H., Friend, R. H. & Silva, C. Electric field-induced transition from heterojunction to bulk charge recombination in bilayer polymer light-emitting diodes. *Appl. Phys. Lett.* **86**, 163501 (2005).
26. Morgado, J., Moon, E., Friend, R. H. & Cacialli, F. Optical and morphological investigations of non-homogeneity in polyfluorene blends. *Synthetic Met.* **124**, 63–66 (2001).
27. Slooff, L. H. *et al.* Near-infrared electroluminescence of polymer light-emitting diodes doped with a lissamine-sensitized Nd^{3+} complex. *Appl. Phys. Lett.* **78**, 2122–2124 (2001).
28. Huang, J. *et al.* Achieving High-Efficiency Polymer White-Light-Emitting Devices. *Adv. Mater.* **18**, 114–117 (2006).
29. Guo, J., Liu, Q., Wang, C. & Zachariah, M. R. Interdispersed Amorphous MnO_x–Carbon Nanocomposites with Superior Electrochemical Performance as Lithium-Storage Material. *Adv. Funct. Mater.* **22**, 803–811 (2012).

30. Brown, T. M. *et al*. Efficient electron injection in blue-emitting polymer light-emitting diodes with LiF/Ca/Al cathodes. *Appl. Phys. Lett.* **79**, 174–176 (2001).
31. Hsiao, Y.-S., Whang, W.-T., Chen, C.-P. & Chen, Y.-C. High-conductivity poly(3,4-ethylenedioxythiophene):poly(styrene sulfonate) film for use in ITO-free polymer solar cells. *J. Mater. Chem.* **18**, 5948–5955 (2008).
32. Antoniadis, H., Abkowiez, M. A. & Hsieh, B. R. Carrier deep-trapping mobility-lifetime products in poly(p-phenylene vinylene). *Appl. Phys. Lett.* **65**, 2030–2032 (1994).
33. Campbell, A. J. *et al*. Transient and steady-state space-charge-limited currents in polyfluorene copolymer diode structures with ohmic hole injecting contacts. *Appl. Phys. Lett.* **76**, 1734–1736 (2000).
34. Chang, H. *et al*. A Transparent, Flexible, Low-Temperature, and Solution-Processible Graphene Composite Electrode. *Adv. Funct. Mater.* **20**, 2893–2902 (2010).
35. Kylberg, W. *et al*. Woven Electrodes for Flexible Organic Photovoltaic Cells. *Adv. Mater.* **23**, 1015–1019 (2011).
36. Jang, J. *et al*. Optoelectronic Characteristics of HgSe Nanoparticle Films Spin-Coated on Flexible Plastic Substrates. *Jpn, J. Appl. Phys.* **49**, 030210 (2010).
37. Jun, J. H., Park, B., Cho, K. & Kim, S. Flexible TFTs based on solution-processed ZnO nanoparticles." *Nanotechnology* **20**, 505201 (2009).
38. Kim, S. Y., Lee, J.-L., Kim, K.-B. & Tak, Y.-H. Effect of ultraviolet–ozone treatment of indium–tin–oxide on electrical properties of organic light emitting diodes. *J. Appl. Phys.* **95**, 2560 (2004).
39. Yun, J., Cho, K. & Kim, S. Flexible logic circuits composed of chalcogenide-nanocrystal-based thin film transistors. *Nanotechnology* **21**, 235204 (2010).

Acknowledgments

This research was supported by the Future-based Technology Development Program (Nano Fields) (NRF-2007-2002746), the Basic Science Research Program (NRF-2013R1A1A2042104), the Mid-career Researcher Program (NRF-2012R1A2A2A01045613) through the National Research Foundation of Korea (NRF) funded by the Ministry of Education, Science and Technology, and a grant from Samsung Display Co., Ltd.

Author contributions

S.K. analyzed the experimental results and wrote the manuscript. K.C. contributed to preparation of the organic materials as well as transparent flexible films, and prepared manuscript. K.K. fabricated all samples and conducted the experiments, and analyzed the experimental data. All authors analyzed and discussed the experimental results.

Additional information

Competing financial interests: The authors declare no competing financial interests.

How to cite this article: Kwak, K., Cho, K. & Kim, S. Stable Bending Performance of Flexible Organic Light-Emitting Diodes Using IZO Anodes. *Sci. Rep.* **3**, 2787; DOI:10.1038/srep02787 (2013).

This work is licensed under a Creative Commons Attribution-NonCommercial-NoDerivs 3.0 Unported license. To view a copy of this license, visit http://creativecommons.org/licenses/by-nc-nd/3.0